ISSN 1674-1056
http://cpb.iphy.ac.cn
http://iopscience.iop.org/cpb
中国物理 B
Chinese Physics
中国物理
Chinese Physics B

Reconstruction of dynamic structures of experimental setups based on measurable experimental data only

Tian-Yu Chen(陈天宇), Yang Chen(陈阳), Hu-Jiang Yang(杨胡江), Jing-Hua Xiao(肖井华), Gang Hu(胡岗)
Citation: Chin. Phys. B . 2018, 27(3): 030503. **doi:** 10.1088/1674-1056/27/3/030503

Journal homepage: http://cpb.iphy.ac.cn; http://iopscience.iop.org/cpb

What follows is a list of articles you may be interested in

Controllable optical superregular breathers in the femtosecond regime

Yang Ren(任杨), Zhan-Ying Yang(杨战营), Chong Liu(刘冲), Wen-Li Yang(杨文力)
Chin. Phys. B . 2018, 27(1): 010504. **doi:** 10.1088/1674-1056/27/1/010504

Constant evacuation time gap:Experimental study and modeling

Ning Guo(郭宁), Rui Jiang(姜锐), Mao-Bin Hu(胡茂彬), Jian-Xun Ding(丁建勋)
Chin. Phys. B . 2017, 26(12): 120506. **doi:** 10.1088/1674-1056/26/12/120506

Relating Maxwell's demon and quantitative analysis of information leakage for practical imperative programs

Kushal Anjaria, Arun Mishra
Chin. Phys. B . 2017, 26(10): 100507. **doi:** 10.1088/1674-1056/26/10/100507

Prompt efficiency of energy harvesting by magnetic coupling of an improved bi-stable system

Hai-Tao Li(李海涛), Wei-Yang Qin(秦卫阳)
Chin. Phys. B . 2016, 25(11): 110503. **doi:** 10.1088/1674-1056/25/11/110503

Computational studies on the interactions of nanomaterials with proteins and their impacts

An De-Yi, Su Ji-Guo, Li Chun-Hua, Li Jing-Yuan
Chin. Phys. B . 2015, 24(12): 120504. **doi:** 10.1088/1674-1056/24/12/120504

Reconstruction of dynamic structures of experimental setups based on measurable experimental data only

Tian-Yu Chen(陈天宇)[1], Yang Chen(陈阳)[1], Hu-Jiang Yang(杨胡江)[1], Jing-Hua Xiao(肖井华)[1,†], and Gang Hu(胡岗)[2,‡]

[1] *School of Science, Beijing University of Posts and Telecommunications, Beijing* 100876, *China*
[2] *Department of Physics, Beijing Normal University, Beijing* 100875, *China*

(Received 30 November 2017; revised manuscript received 4 January 2018; published online 13 February 2018)

Nowadays, massive amounts of data have been accumulated in various and wide fields, it has become today one of the central issues in interdisciplinary fields to analyze existing data and extract as much useful information as possible from data. It is often that the output data of systems are measurable while dynamic structures producing these data are hidden, and thus studies to reveal system structures by analyzing available data, i.e., reconstructions of systems become one of the most important tasks of information extractions. In the past, most of the works in this respect were based on theoretical analyses and numerical verifications. Direct analyses of experimental data are very rare. In physical science, most of the analyses of experimental setups were based on the first principles of physics laws, i.e., so-called top-down analyses. In this paper, we conducted an experiment of "Boer resonant instrument for forced vibration" (BRIFV) and inferred the dynamic structure of the experimental set purely from the analysis of the measurable experimental data, i.e., by applying the bottom-up strategy. Dynamics of the experimental set is strongly nonlinear and chaotic, and it's subjects to inevitable noises. We proposed to use high-order correlation computations to treat nonlinear dynamics; use two-time correlations to treat noise effects. By applying these approaches, we have successfully reconstructed the structure of the experimental setup, and the dynamic system reconstructed with the measured data reproduces good experimental results in a wide range of parameters.

Keywords: dynamics, inverse problem, data analysis

PACS: 05.45.Tp, 05.45.–a **DOI:** 10.1088/1674-1056/27/3/030503

1. Introduction

In recent years, a large scale of data has been accumulated in various fields, especially in social and biological systems.[1–4] However, the system structures generating these data are usually not clear.[5,6] Therefore, it is very important in interdisciplinary fields to reveal system structures by analyzing their output data, called dynamic structure reconstructions.[7–13] A typical example in this regard is a recent dialogue project on reverse engineering assessment and methodology (DREAM), which has attracted considerable attention in the field of reconstructing gene regulatory networks.[14,15] Similar objectives are found in other areas, such as neural networks[16,17] and ecosystems.[18] Mathematically, dynamics of systems considered are widely described as coupling ordinary differential equations (ODEs),[19–22] and the problem of system reconstructions is thus to reveal these linear or nonlinear structures of the differential systems. So far, many system structures' reasoning methods had been proposed to different fields to solve various structure reconstruction problems.[15,23–27] In most of the practical cases, network reconstructions from measurable data must encounter some major difficulties: nonlinearity of network dynamics; and effects of unknown impacts, such as noise. The joint interplay of these difficulties makes the problem of network reconstructions challenging. In order to overcome these difficulties, some new integrated physical thinking and intelligent methods have been proposed.[15,23–34] So far, most of the works of network reconstructions have considered mathematical analyses and numerical simulations of various models, and much fewer works directly analyzed realistic experimental data. Moreover, a majority of works of network reconstructions are in the social and biological disciplines. In physics, scientists have been familiar with research strategies, starting from the first principles, i.e., so-called top-down analyses, and people have very seldom inferred structures of experimental setups by analyzing measurable data of experiments only. Due to some unknown complexities of experimental sets; unknown experimental surrounding; and strong nonlinearity and chaotic of dynamics, the conventional top-down strategies are not always successful, and direct analyses of experimental data, i.e., the bottom-up strategies, may serve as useful tools to reconstruct experimental structures. In this paper, we collect data of oscillating angle of the Boer resonant instrument under forced vibration with a very high measurement frequency and try to reveal the dynamical structure of the experimental set purely from measurable data. For performing effective data analysis, we use high-order correlations to treat nonlinearity of the experimental system, and two-time correlations to deal with noises existing in the

†Corresponding author. E-mail: jhxiao@bupt.edu.cn
‡Corresponding author. E-mail: ganghu@bnu.edu.cn

© 2018 Chinese Physical Society and IOP Publishing Ltd

experiment. Then by analyzing the available angle data only, we are able to infer the interaction structures between different experimental subsets; fix some unknown and not measurable physical parameters, and reconstruct the dynamic model of the experimental system. In particular, the reconstructed mechanical model can satisfactorily reproduce essential dynamic features in a wide range of control parameters, though the data under analysis are taken from the experimental measurement at a fixed single parameter set.

2. Experimental setup and data measurements

In this paper, we conduct an experiment of "Boer resonant instrument for forced vibration", i.e., we use a fine iron bar with a matching nut adding on a Pohl's torsion pendulum to complicate the apparatus,[35] and further, introduce a double-well potential into the basic torsion pendulum apparatus. This experimental setup can produce very rich experiment results such as complicated patterns of periodic and chaotic motions and diverse bifurcations between these patterns, by varying a single experimental parameter, the frequency of the driving force, only.[36–39]

2.1. Device setup

Pohl's torsion pendulum is a torsional harmonic oscillator that can oscillate with a rotational motion about the axis of a torsion spring clockwise and counterclockwise. Its behaviors are analogous to those of translational spring-mass oscillators, and the corresponding linear iZed equation of the copper rotating wheel is accepted for describing its dynamics, which is

$$J\frac{\mathrm{d}^2\theta}{\mathrm{d}t^2}+\gamma\frac{\mathrm{d}\theta}{\mathrm{d}t}+k\theta=M\cos\frac{2\pi}{T}t, \tag{1}$$

where J is the moment inertia of the copper rotating wheel, γ is the friction parameter, k is the stiffness coefficient of the convoluted spring, G is the amplitude of the driving torque, and T is the driving period. Such apparatus can support only very simple periodic motion, and cannot be used to explain complicated nonlinear dynamic phenomena such as chaotic patterns and transitions between different types of motions. To overcome this flaw, the linear oscillator is modified into various nonlinear oscillators by adding various nonlinear terms to the rotating wheel, and the set in Fig. 1 is one of them. In Fig. 1, we add a fine iron bar with a matching nut in the vertical direction going through the center of the copper rotating wheel, which provides nonlinear factors of the system. Specifically, the parameters of mass quality, diameter, and length of the fine iron bar are set at 19.4 g, 4.8 mm, and 155 mm, respectively, and the mass of the nut is fixed to 2.1 g. One can easily change the nonlinear torque continuously by adjusting the position of the nut on the iron bar. A number of works have studied such an experimental setup and modeled the system by

$$J'\frac{\mathrm{d}^2\theta}{\mathrm{d}t^2}+\gamma\frac{\mathrm{d}\theta}{\mathrm{d}t}+k\theta=M\cos\frac{2\pi}{T}t+mgr\sin\theta, \tag{2}$$

where m is the total mass of the fine iron bar and the matching nut (nonlinear component), and g is the gravity acceleration, and r is the distance between the barycenter of the iron bar with matching nut and the center of the rotating wheel. In experiments (Fig. 1), we can freely adjust period T (i.e., frequency $1/T$) and damping item γ by adjusting the periodic driving tuner and the damping

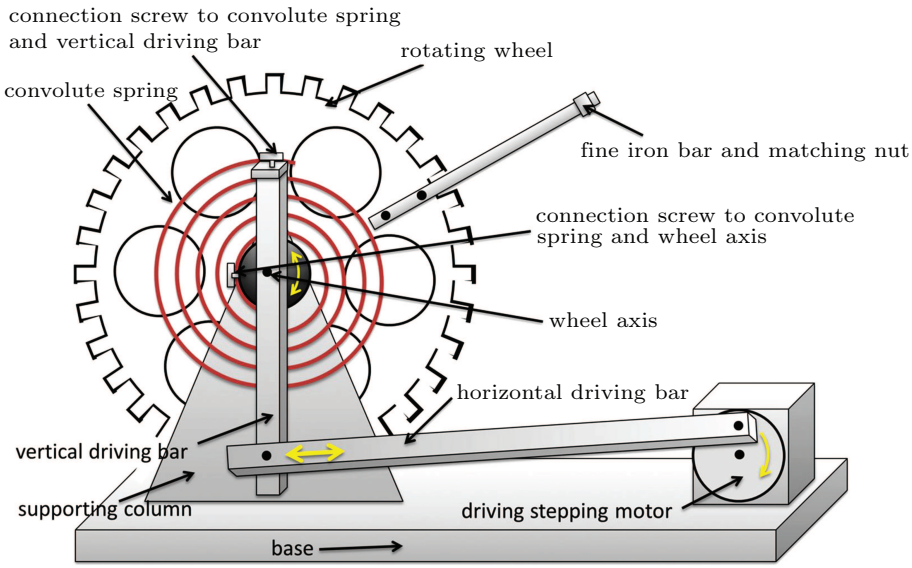


Fig. 1. (color online) Experimented setup of "Boer resonant instrument for forced vibration",[35] a fine iron bar with a matching nut is added to a Pohl's torsion pendulum, and a double-well potential structure is introduced by a torsion pendulum apparatus through adding weights to the copper rotating wheel of Pohl's torsion pendulum basis. Extremely rich experiment results can be explored in the torsion pendulum experiment, including rich patterns of periodic and chaotic motions and diverse bifurcations between these patterns, by varying a single experimental parameter, the frequency of the driving force, only.

controller. By shifting the position of the matching nut on the fine iron bar, the parameter γ can be changed on purpose, that modifies the depth of the double-well potential. With these modifications, the modified Pohl's torsion pendulum can exhibit rich nonlinear behaviors of periodicities, chaoticities, and various bifurcations between different patterns.

2.2. Data collection and dynamic phenomena

In all experiments, the data of swing angle θ are measured by an organic glass turntable and collected. The frequency of measurements are very high as $f_{\rm m} = 50$ Hz, and the duration of angle measurement is rather long up to $L = 7200$ s, so that all behaviors of different types of motions can be well captured. By recording the swing angle for different driving periods, complicated bifurcation diagrams of θ, responding to changes of parameter T are manifested. In Fig. 2, we show some typical patterns of θ trajectories where periodic and chaotic motions are observed at different parameters. Figure 3 shows the bifurcation pattern in the experimental data against the variation of the driving frequency with all other parameters fixed. Note that all plots in Figs. 2 and 3 are presented purely from the measured experimental data. Fast-varying as well as noisy impacts are obviously observed, for all periodic and chaotic trajectories in Fig. 2 have wide widths and fast-varying fluctuations. Equation (2) can be regarded as being derived from the first principles of the analysis of mechanisms of experimental set, i.e., from the top-down strategy. A number of problems are not solved by Eq. (2). First, some parameters, like friction γ and spring constant k, may be unknown. Second and most important, the dynamic form prior assumed in Eq. (2) may not be

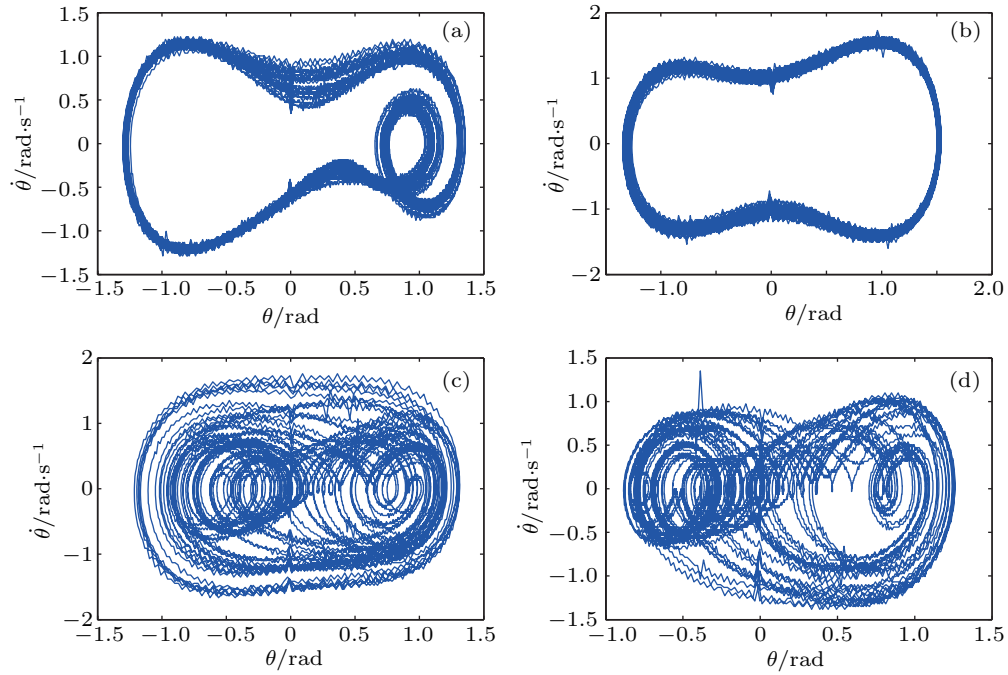


Fig. 2. (color online) By changing the driving period, the θ motion of the BRIFV experiment transits between rich patterns of periodic and chaotic motions. (a) $T = 10.42$ s, (b) $T = 5.38$ s, (c) $T = 3.27$ s, and (d) $T = 2.60$ s.

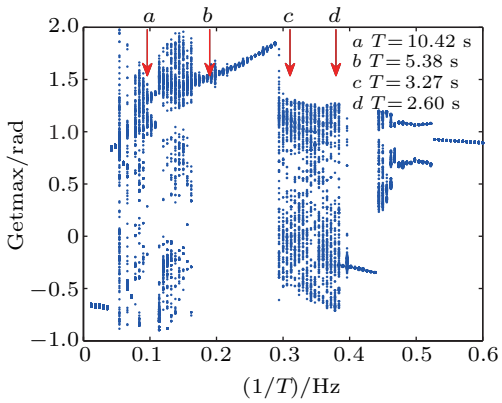


Fig. 3. (color online) Bifurcation diagram of the experimental setup in Fig. 1, plotted by data at time moments $t = kT$, $k \geq 2300$. "Getmax" means the max angle in period T. A rich and fine bifurcation structure is observed by varying periods of the driving and fixing all other parameters the same as these in Fig. 2.

correct, and other complicated and unknown nonlinear facts not included in Eq. (2) may essentially affect the experimental dynamics. In this paper, we adopt purely bottom-up strategy of the investigation. Namely, we assume that all parameters of Eq. (2), and even the form of Eq. (2) itself are unknown, and we have a task to explore the dynamic structure underlying the experimental processes purely from the measurable θ data through standard dynamics reconstruction procedures explained in the next section.

3. Formula derivation of dynamic structure reconstruction

In this section, we consider the dynamics structure reconstruction of the experimental sets (Fig. 1) from the measured

data (Figs. 2 and 3). First, we describe the general theory for the reconstruction.

Since phase angle data $\theta(t)$ of the BRIFV set are collected, the rule governing the pendulum evolution can be generally written as

$$\ddot{\boldsymbol{\theta}}(t) = \boldsymbol{F}(\dot{\theta}(t),\theta(t),t) + \boldsymbol{\Gamma}(\boldsymbol{t}), \tag{3}$$

where noise term $\boldsymbol{\Gamma}(t)$ is assumed from microscopic impacts, which varies much faster than the time scale of pendulum dynamics (see Fig. 2 for the evidence), and can be approximated as white noise

$$\langle \boldsymbol{\Gamma}(t)\rangle = 0, \langle \boldsymbol{\Gamma}(t)\boldsymbol{\Gamma}(t')\rangle = D(\theta)\sigma(t-t'). \tag{4}$$

Both field $\boldsymbol{F}$ and noise intensity $D(\theta)$ are unknown. The frequency of deterministic periodic driving can be controlled and known while the amplitude (which may or may not be θ dependent) of driving and all the other dependencies of $\boldsymbol{F}$ on θ and $\dot{\theta}$ are unknown. The central task of this section is to infer an explicit form of $\boldsymbol{F}(\dot{\theta},\theta,t)$ from available data $\theta(t)$ only.

This task can be formally done as follows. By expanding $\boldsymbol{F}$ on a certain function basis set as

$$\boldsymbol{F}(\dot{\theta}(t),\theta(t),t) = \sum_{i=1}^{M} F_i \boldsymbol{Z}_i(\dot{\theta}(t),\theta(t),\cos(\omega t),\sin(\omega t)), \tag{5}$$

with $\boldsymbol{Z}_i$ being known functions of $\dot{\theta}(t)$, $\theta(t)$, $\cos(\omega t)\sin(\omega t)$. Defining the partner basis set $\bar{\boldsymbol{Z}}_i'(\dot{\theta}(t),\ \theta(t),\ \cos(\omega t),\ \sin(\omega t))$, $i = 1,2,\ldots,M$, and multiplying both sides of Eq. (3) by partner bases $\boldsymbol{Z}'^{\mathrm{T}}(t-\tau)$; (the transposition of vector Z') and computing all related connections, we arrive at a set of algebraic equations

$$\boldsymbol{B} = \boldsymbol{F}\widehat{\boldsymbol{C}} + \langle \boldsymbol{\Gamma}(t)\boldsymbol{Z}'(t-\tau)\rangle, \tag{6}$$

where constant vector $\boldsymbol{F}$ given in Eq. (5) as

$$\boldsymbol{F} = (F_1 F_2,\ldots,F_M), \tag{7a}$$

vector $\boldsymbol{B}$ is computable from data

$$\begin{aligned} &\boldsymbol{B} = (B_1,B_2,\ldots,B_M),\\ &B_i = \frac{1}{L-\dfrac{\tau}{\Delta t}}\sum_{k=\frac{\tau}{\Delta t}+1}^{L} \ddot{\theta}_k(t_k) Z_i(\dot{\theta}(t_{k-\frac{\tau}{\Delta t}}),\theta(t_{k-\frac{\tau}{\Delta t}}),t_{k-\frac{\tau}{\Delta t}}), \end{aligned} \tag{7b}$$

and matrix $\widehat{\boldsymbol{C}}$ is computable as well from the measured data as

$$\begin{aligned} \widehat{\boldsymbol{C}} &= (C_{ij}),\quad i,j = 1,2,\ldots,M,\\ C_{ij} &= \frac{1}{L-\dfrac{\tau}{\Delta t}}\sum_{k=\frac{\tau}{\Delta t}+1}^{L} Z_i(\dot{\theta}(t_k),\theta(t_k),t_k)\\ &\quad\times Z_j(\dot{\theta}(t_{k-\frac{\tau}{\Delta t}}),\theta(t_{k-\frac{\tau}{\Delta t}}),t_{k-\frac{\tau}{\Delta t}}). \end{aligned} \tag{7c}$$

In Eq. (6), the last correlation should vanish

$$\langle \boldsymbol{\Gamma}(t)\boldsymbol{Z}(t-\tau)\rangle \approx 0, \tag{8}$$

because of the approximation in Eq. (4), for any fast-varying noise at time t is not correlated to any variable functions at earlier time $t-\tau$ with τ being larger than the correlation time of noise.

If all terms in Eqs. (7) and (8) are identified, equation (6) can be thus explicitly computed as

$$\boldsymbol{B} = \boldsymbol{F}\widehat{\boldsymbol{C}},$$

leading to

$$\boldsymbol{F} = \boldsymbol{B}\widehat{\boldsymbol{C}}^{-1}. \tag{9}$$

Since all elements of $\boldsymbol{B}$ and $\widehat{\boldsymbol{C}}$ are computable with measured data $\theta(t)$, dynamic structure of $\boldsymbol{F}$ in Eq. (5) can be inferred. In the remaining part of this paper, we simply use identical expansions for the basis set $\boldsymbol{Z}'$ and partner set $\boldsymbol{Z}'$

$$Z_i(\dot{\theta}(t),\theta(t),t) = Z'(\dot{\theta}(t),\theta(t),t),\quad i = 1,2,\ldots,M.$$

Up to now, there are still several points to be made clear before Eq. (9) can be used in the realistic reconstruction of experimental set. First, one has to choose proper bases in Eq. (5) for field expansion; second, it is crucial to choose suitable truncation M for fixing basis set, too large M can be too computationally consuming and can cause low reconstruction accuracy while too small M may give wrong reconstruction results; third, in Eq. (9) one has to compute the inverse of matrix $\widehat{\boldsymbol{C}}$, and thus this $\widehat{\boldsymbol{C}}$ should be invertible. Any singularities (zero eigenvalues) of matrix $\widehat{\boldsymbol{C}}$ can make the inverse computation fail. These problems will be treated one by one as follows.

i) Since we are considering a pendulum system and measuring phase angle $\theta(t)$ as our data, Fourier expansion can serve as suitable expansion bases, and equation (3) can be very generally specified as

$$\begin{aligned} \ddot{\theta}(t) &= \sum_{i_1=1}^{m_1}(F_{i_1}\cos(i_1\theta) + F_{i_1+m_1}\sin(i_1\theta))\dot{\theta} + F_{2m+1}\dot{\theta}\\ &\quad + \sum_{i_2=1}^{m_2}(F_{i_2+2m_1}\cos(i_2\theta) + F_{i_2+2m_1+m_2}\sin(i_2\theta))\\ &\quad + \sum_{i_3=1}^{m_3}(F_{i_3+2m_1+2m_2}\cos(i_3\theta)\\ &\quad + F_{i_3+2m_1+2m_2+m_3}\sin(\mathrm{i}_3\theta))\cos(wt)\\ &\quad + \sum_{i_3=1}^{m_3}(F_{i_3+2m_1+2m_2+2m_3}\cos(i_3\theta)\\ &\quad + F_{i_3+2m_1+2m_2+3m_3}\sin(i_3\theta))\sin(wt)\\ &\quad + F_{2m_1+2m_2+4m_3+1}. \end{aligned} \tag{10}$$

In Eq. (10), the terms multiplied by $\dot{\theta}$ represent friction effects which may or may not be angle-dependent in the given experiment. The terms of pure Fourier expansion provides possible choices for the angle-dependent potential. The last part of terms multiplied by $\cos(wt)$ and $\sin(wt)$ show the general form of periodic driving.

ii) In Eq. (10), suitable truncations m_1,m_2,m_3 (or the total truncation $M = 2m_1+2m_2+4m_3+1$) are to be determined,

and both too large or too small truncations can seriously influence the quality of structure reconstruction. For seeking proper truncations, we apply the compressive sensing (CS) method.[40] The main idea is to adapt a sparse approximation algorithm called orthogonal matching pursuit (OMP),[41,42] to handle the signal recovery problem and to choose suitable terms for the computation of Eq. (9).

iii) After truncation M is fixed in Eq. (5), $\widehat{C}$ matrix in Eq. (9) can be computed. If $\widehat{C}$ has some zero (or near to zero) eigenvalues, some linear correlation relations exist between some vector bases, and one has to delete some bases one by one until $\widehat{C}$ becomes invertible.

Considering all the above three items, a well-defined and closed algorithm Eqs. (5), (7), and (9) with a suitably chosen truncation M can be conducted. In our experiment and with the available data collected in the chaotic regime, we adopt the following candidate system, based on the results of CS:

$$\begin{aligned}\ddot{\theta}(t) &= F_1\dot{\theta} + F_2\cos(\omega t) + F_3\sin(\omega t) + F_4\cos(\theta)\\ &\quad + F_5\sin(\theta) + F_6\cos(2\theta) + F_7\sin(2\theta)\\ &\quad + F_8\cos(3\theta) + F_9\sin(3\theta),\end{aligned} \tag{11}$$

and $\boldsymbol{Z}$ and $\boldsymbol{F}$ can be specified as

$$\begin{aligned}\boldsymbol{Z} &= (\dot{\theta}, \cos(\omega t), \sin(\omega t), \cos(\theta), \sin(\theta),\\ &\quad \cos(2\theta), \sin(2\theta), \cos(3\theta), \sin(3\theta)),\\ \boldsymbol{F} &= (F_1, F_2, F_3, F_4, F_5, F_6, F_7, F_8, F_9).\end{aligned} \tag{12}$$

4. Data analysis and structure reconstruction

Using the data collected from the chaotic states at different T's of Fig. 3 and computing Eq. (9) with the basis set in Eq. (11), we can reconstruct all different parameter sets of Eq. (11), and thus reconstruct a model system to represent the dynamics of the experimental set (Fig. 1).

In order to justify the sufficiency of M truncation in Eq. (11), we can apply a self-consistent checking method.[43] After inferring structure $\boldsymbol{F}$ with the truncation of Eq. (11), we further consider a truncation $M' > M$ to infer structure of $\boldsymbol{F}'$. M' includes all bases in Eq. (11), and adds some more bases with slightly lower ranks in CS basis sequence. If $\boldsymbol{F}$ of M truncation is identically reproduced in $\boldsymbol{F}'$ with M' truncation, and if all other parameters $F_{M+i}, i = 1, 2, \ldots, M' - M$, not included in Eq. (11) are approximately zero, the reconstruction of M truncation of Eq. (11) is self-consistently justified. In Fig. 4, we plot $\boldsymbol{F}'$ against $\boldsymbol{F}$ where both $\boldsymbol{F}'$ and $\boldsymbol{F}$ are computed by applying Eq. (9) with data collected in several experiments at different T in the range of 0078 s–0.198 s. M is given by Eq. (11) and M' includes all bases of Eq. (11) and two other bases of $\cos(6\theta)$ and $\sin(6\theta)$. All dots, representing the M parameters in Eq. (11) computed in both $\boldsymbol{F}$ and $\boldsymbol{F}'$, are around the diagonal line and all parameters included in $\boldsymbol{F}'$ while not included in the bases of Eq. (11) are nearly zero (red circles in Fig. 4(a)). These results support convincingly the structure reconstruction of Eqs. (9) and (11). In Fig. 4(b), we do something just opposite, i.e., we decrease truncation numbers M from Eq. (11) to $M' = 7$ by deleting the terms of $\cos(2\theta), \sin(2\theta)$, and do the same thing as that in Fig. 4(a). Dots distribute considerably away from the diagonal line, indicating $M' = 7$ used here is not a suitable truncation.

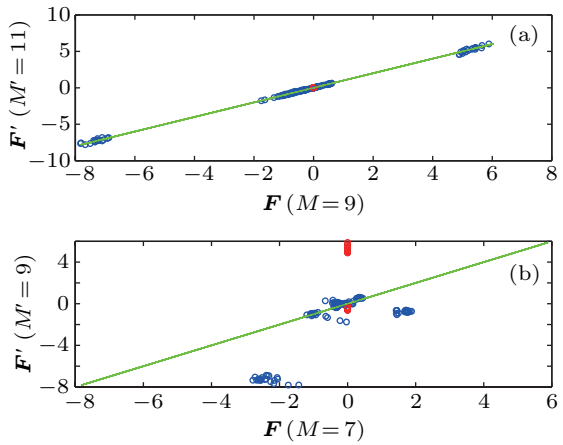


Fig. 4. (color online) (a) and (b) Parameters reconstructed with 2 different truncations M's (vertical lines) plotted against those reconstructed by M truncation adopted in Eq. (11). $M' > M$ ($M' = 11$, $\boldsymbol{Z}_{M'} = (\dot{\theta}, \cos(\omega t), \sin(\omega t), \cos(\theta), \sin(\theta), \cos(2\theta), \sin(2\theta), \cos(3\theta), \sin(3\theta), \cos(6\theta), \sin(6\theta))$, $\boldsymbol{F} = (F_1, F_2, F_3, F_4, F_5, F_6, F_7, F_8, F_9, F_{10}, F_{11})$) and M' includes all M parameters of Eq. (11), all dots are around the diagonal line and all parameters not included in the M of Eq. (11) bases are nearly zero (red circles), justifying the sufficiency of truncation of Eq. (11). (b) The same as panel (a) with two terms of $\cos(2\theta), \sin(2\theta)$ in Eq. (11) deleted ($M = 7$, $\boldsymbol{Z}_M = (\dot{\theta}, \cos(\omega t), \sin(\omega t), \cos(\theta), \sin(\theta), \cos(3\theta), \sin(3\theta))$, $\boldsymbol{F} = (F_1, F_2, F_3, F_4, F_5, F_6, F_7)$. Dots distribute considerably away from the diagonal line, concluding such truncation of $M = 7$ not suitable.

With parameters reconstructed by using Eqs. (9) and (11), we can model the dynamics of the experimental set by using Eq. (11), i.e., we can numerically run Eq. (11) and compare the data of simulations with data directly collected by experimental measurements. In Fig. 5, we use different data sets collected in experiments at four different periods of Fig. 2, and reconstruct parameters of Eq. (11), and numerically run Eq. (11) and produce bifurcation figures as we did for experimental data from the experiments for different and fixed $T's$ in Fig. 3. It is surprising that though parameters in the four figures are obtained from experimental data collected at different and fixed $T's$, the whole bifurcation structure observed in experiment Fig. 3 for a large range of T is fully (approximately, of course) reproduced in all the four figures. A number of characteristic features such as distributions of periodic regions, chaotic domains, and transitions between different patterns appearing in the four reconstructed nonlinear systems (Fig. 5) are rather similar and all of them are similar to the experimental results of Fig. 3 with certain fluctuation and shifted distributions.

In Fig. 6, we do exactly the same as that in Fig. 2, with the trajectories produced by numerical simulations of Eq. (11) with parameters of Fig. 5(a). The four pairs of experimental (Fig. 2) and numerical (Fig. 6) trajectories are rather simi-

lar to their periodicity, chaoticity and the trajectory structures, though all four trajectories in Fig. 6 are reproduced by Eq. (11) with parameters reconstructed with an experimental data set collected at a single fixed period $T = 10.42$ s. It is emphasized that the experimental data of periodic orbits are not very good for structure inference (see Fig. 5(b)) because periodic data have low dimensionality and include less information than those of chaotic states. On the other hand, data from different fully chaotic states can be used for the reconstruction task, and data collected at different driving frequencies can equally and rather robustly reproduce experimental behaviors as shown in Figs. 5(a), 5(c), and 5(d).

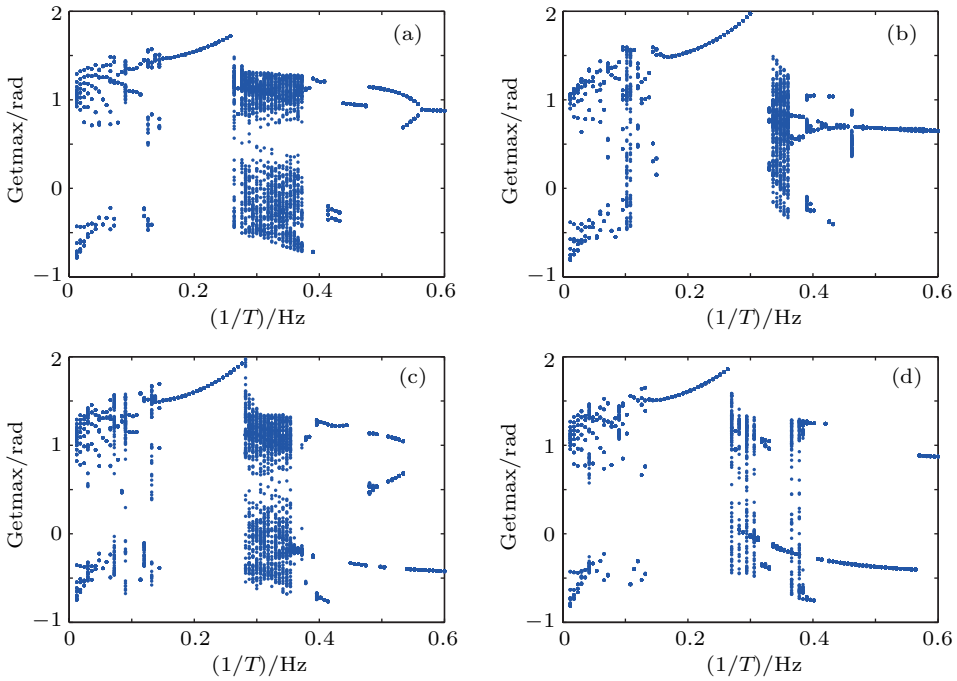


Fig. 5. (color online) Numerical results of constructed Eq. (11). Four figures use parameters reconstructed with four data sets collected in experiments at $T = 10.42$ s (a), 5.38 s (b), 3.27 s (c), and 2.60 s (d), respectively. T step for producing numerical results is the same as that of the experiment, $\Delta t = 0.05$ s. A number of characteristic features such as distributions of periodic regions, chaotic domains and their turning points of the four reconstructed systems are rather similar to each other and all of them show essential features of the experimental results of Fig. 3.

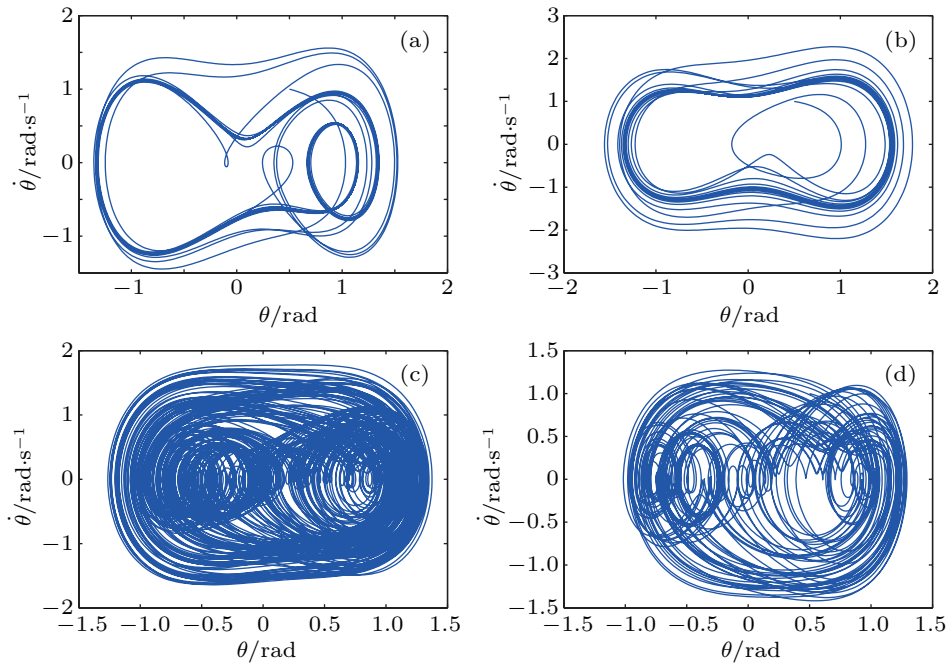


Fig. 6. (color online) The same as Fig. 2, with trajectories produced by numerical simulations of Eq. (11) using parameters reconstructed in Fig. 5(a). (a) $T = 10.42$ s, (b) 5.38 s, (c) 3.27 s, and (d) 2.60 s (the same as these in Figs. 2(a)–2(d), respectively). The four pairs of experimental (Fig. 2) and numerical (Fig. 6) trajectories are rather similar to their periodicity, chaoticity and the trajectory structures, though all four trajectories in Fig. 6 are reproduced by Eq. (11) with parameters reconstructed with an experimental data set collected at a single fixed period $T = 10.42$ s.

5. Conclusion

In conclusion, we have performed the dynamic structure reconstruction of an experimental set "Boer resonant instrument for forced vibration" based on measured experimental data only. So far, most of the works on the system reconstructions have considered various model systems. In this paper, the systematical analysis fully based on experimental data will be useful for practical applications in wide fields. In physics, we are familiar with various derivations, starting from physical first principles, i.e., a top-down investigation strategy. In this paper, we assume no prior knowledge of the experimental structure, except some general and well-known understanding of friction, driving and angle property of measured data. Purely from experimentally measured data, we can infer the structure of the experimental set. This bottom-up strategy can explore not only the "first principles", i.e., the main dynamic structure, of the experiment, but also reveal the concrete parameter values in the experimental set, which cannot be directly derived from the first principles. In Figs. 5 and 6, we show that the dynamic systems reconstructed from experimental data sets can produce numerical data having features rather similar to those of the experimental data, and can predict experimental behaviors at conditions where no data measurement has been conducted. This prediction is possible only as both physical principles and detailed parameter reconstructions are explored. Both top-down and bottom-up investigation strategies are important in exploring system structures. We hope that jointly combining these two strategies in many practical systems may provide powerful tools in reconstructions of realistic systems.

References

[1] Butte A J, Tamayo P, Slonim D, Golub T R and Kohane I S 2000 *Proc. Natl. Acad. Sci.* **97** 12182

[2] Kim S K, Lund J, Kiraly M, Duke K, Jiang M, Stuart J M, Eizinger A, Wylie B N and Davidson G S 2001 *Science* **293** 2087

[3] Bar-Joseph Z, Gerber G K, Lee T I, Rinaldi N J, Yoo J Y, Robert F, Gordon D B, Fraenkel E, Jaakkola T S, Young R A and Gifford D K 2003 *Nat. Biotechnol.* **21** 1337

[4] Bar-Joseph Z, Gitter A and Simon I 2012 *Nat. Rev. Genet.* **13** 552

[5] Feist A M, Herrgard M J, Thiele I, Reed J L and Palsson B O 2009 *Nat. Rev. Microbiol.* **7** 129

[6] De Smet R and Marchal K 2010 *Nat. Rev. Microbiol.* **8** 717

[7] Yeung M S, Tegnér J and Collins J J 2002 *Proc. Natl. Acad. Sci.* **99** 6163

[8] Stuart J M, Segal E, Koller D and Kim S K 2003 *Science* **302** 249

[9] Segal E, Shapira M, Regev A, Pe'er D, Botstein D, Koller D and Friedman N 2003 *Nat. Genet.* **34** 166

[10] Hu Z, Killion P J and Iyer V R 2007 *Nat. Genet.* **39** 683

[11] Lezon T R, Banavar J R, Cieplak M, Maritan A and Fedoroff N V 2006 *Proc. Natl. Acad. Sci.* **103** 19033

[12] Barzel B and Barabási A L 2013 *Nat. Biotechnol.* **31** 720

[13] Feizi S, Marbach D, Médard M and Kellis M 2013 *Nat. Biotechnol.* **31** 726

[14] Marbach D, Prill R J, Schaffter T, Mattiussi C, Floreano D and Stolovitzky G 2010 *Proc. Natl. Acad. Sci.* **107** 6286

[15] Marbach D, Costello J C, Küffner R, Vega N M, Prill R J, Camacho D M, Allison K R, The DREAM5 Consortium, Kellis M, Collins J J and Stolovitzky G 2012 *Nat. Methods* **9** 796

[16] Bullmore E and Sporns O 2009 *Nat. Rev. Neurosci.* **10** 186

[17] Burioni R, Casartelli M, Di Volo M, Livi R and Vezzani A 2014 *Sci. Rep.* **4** 4336

[18] Sugihara G, May R, Ye H, Hsieh C H, Deyle E, Fogarty M and Munch S 2012 *Science* **338** 496

[19] Glass L and Mackey M C 1988 *From Clocks to Chaos: the Rhythms of Life* (Princeton: Princeton University Press)

[20] Goldbeter A and Tyson J J 1996 *Nature* **380** 213

[21] Alon U 2006 *An introduction to Systems Biology: Design Principles of Biological Circuits* (Boca Raton: CRC Press)

[22] Tsai T Y C, Choi Y S, Ma W, Pomerening J R, Tang C and Ferrell J E 2008 *Science* **321** 126

[23] Basso K, Margolin A A, Stolovitzky G, Klein U, Dalla-Favera R and Califano A 2005 *Nat. Genet.* **37** 382

[24] Bansal M, Belcastro V, Ambesi-Impiombato A and Di Bernardo D 2007 *Mol. Syst. Biol.* **3** 78

[25] Villaverde A F, Ross J and Banga J R 2013 *Cells* **2** 306

[26] Jansen R, Yu H, Greenbaum D, Kluger Y, Krogan N J, Chung S B, Emili A, Snyder M, Greenblatt J F and Gerstein M 2003 *Science* **302** 449

[27] Hao C Q, Wang J, Deng B and Wei X L 2012 *Acta Phys. Sin.* **61** 130507 (in Chinese)

[28] Friedman N 2004 *Science* **303** 799

[29] Gardner T S, Di Bernardo D, Lorenz D and Collins J J 2003 *Science* **301** 102

[30] Eisen M B, Spellman P T, Brown P O and Botstein D 1998 *Proc. Natl. Acad. Sci.* **95** 14863

[31] Faith J J, Hayete B, Thaden J T, Mogno I, Wierzbowski J, Cottarel G, Kasif S, Collins J J and Gardner T S 2007 *PLoS Biol.* **5** e8

[32] Wang W X, Chen Q, Huang L, Lai Y C and Harrison M A F 2009 *Phys. Rev. E* **80** 16116

[33] Ren J, Wang W X, Li B and Lai Y C 2010 *Phys. Rev. Lett.* **104** 58701

[34] Ching E S, Lai P Y and Leung C Y 2013 *Phys. Rev. E* **88** 42817

[35] Miao C, Luo W, Ma Y, Liu W and Xiao J 2014 *Eur. J. Phys.* **35** 55012

[36] Stavrou D, Assimopoulos S and Skordoulis C 2013 *Phys. Educ.* **48** 355

[37] Peters R D 1995 *Am. J. Phys.* **63** 1128

[38] Berger J E and Nunes Jr G 1997 *Am. J. Phys.* **65** 841

[39] Roal'd Zinnurovich Sagdeev, Daniel'Alekseevich Usikov and Zaslavskii G M 1990 *Harwood Academic*

[40] Tropp J A and Gilbert A C 2007 *IEEE Trans. Inf. Theory* **53** 4655

[41] Pati Y C, Rezaiifar R and Krishnaprasad P S 1993 *Conference Record of The Twenty-Seventh Asilomar Conference on Signals, Systems and Computers*, November 1–3, 1993, Pacific Grove, CA, USA, p. 4846193

[42] Davis G, Mallat S and Avellaneda M 1997 *Constr. Approx.* **13** 57

[43] Chen Y, Zhang Z Y, Chen T Y, Wang S S and Hu G 2017 *Sci. Rep.* **7** 44639